INLINE RELATIVE PERMITTIVITY SENSING USING SILICON ELECTRODES REALIZED IN SURFACE CHANNEL TECHNOLOGY

Dennis Alveringh[1], Remco J. Wiegerink[1], and Joost C. Lötters[1,2]
[1] MESA+ Institute for Nanotechnology, University of Twente, Enschede, THE NETHERLANDS
[2] Bronkhorst High-Tech BV, Ruurlo, THE NETHERLANDS

ABSTRACT

Sensing relative permittivity is useful for fluid characterization, since its value differs significantly for different substances. A microfabricated inline relative permittivity sensor is realized using surface channel technology with support for isolated silicon electrodes. This enables non-invasive composition measurements of chemicals, i.e. the chemicals are not in contact with an electrode, do not need to be heated or need to be mixed with a chemical marker. Since this sensor operates inline, real-time measurements of the fluid can be obtained. Besides, integration with other fluid sensors, e.g. flow or pressure sensors, on a single chip could be achieved due to the sensor's full compatibility with surface channel technology. This is the first device that successfully uses the isolated silicon electrode functionality of this fabrication technology. Preliminary measurement results show a high coefficient of determination (R^2 = 99.83 %) with the model.

INTRODUCTION

The relative permittivity can roughly be seen as the resistance of a material against an electric field. Although the relative permittivity might seem to be a very specific quantity that is only interesting for specific electronic purposes, it has interesting properties in a more indirect way. The value varies a lot between fluids. E.g. methanol has a relative permittivity of approximately 30 % higher than ethanol [1], while the transparency and density are quite similar. It has therefore great potential for fluid characterization and composition measurements. Latter method has applications in flow chemistry for the production of chemicals and acurate medication delivery using intravenous therapy.

Not much has been published on relative permittivity sensing of fluids. Some US patents [2, 3, 4, 5, 6] claim different measurement principles, but are all not microfabricated and cannot be integrated with other sensors. The only microfabricated inline relative permittivity sensor is embedded in the system of Lötters et al. [7]. While the paper shows the significance of relative permittivity sensing for fluid characterization and composition measurement, the sensor has a relatively large electrode distance of 50 µm and it has not been modeled in detail. Therefore, dependence on other fluid parameters and parasitic effects are unknown and cannot be compensated for.

THEORY

For linear, homogeneous, isotropic and nondispersive materials as dielectric, the capacitance for a parallel plate

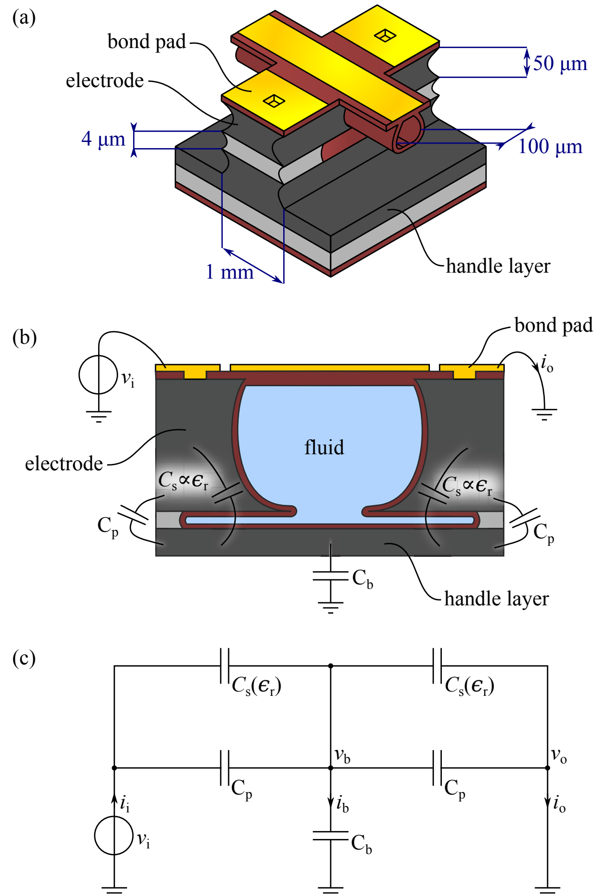

Figure 1: Illustration of the relative permittivity sensor in isometric (a) and cross-sectional view (b). The relative permittivity of the fluid in the microchannel can be obtained by measuring the impedance between the two isolated silicon electrodes, modeled as an electrical circuit in (c).

capacitor is [8]:

$$C_s(\varepsilon_r) = \varepsilon_0 \varepsilon_r \frac{A}{d} = \beta \varepsilon_r, \tag{1}$$

with ε_0 the constant vacuum permittivity, ε_r the relative permittivity, A the surface area of the electrodes and d the distance between the electrodes, all combined in β. As follows directly from this equation, a high sensitivity can be achieved by a high A/d-ratio, i.e. a large electrode area and/or small distance between the electrodes.

Figures 1a and 1b show an illustration of the proposed sensor. A microfluidic channel, with a channel wall of < 1 µm, is realized in the device layer of a silicon-on-insulator wafer and extends sideways into the buried oxide layer. Electrodes are realized at both sides of the channel forming capacitances to the handle layer through the thin channel of fluid. The relative permittivity is found by

measuring the impedance between the silicon electrodes and the silicon handle layer. The impedance is estimated by measuring the transfer from a voltage v_i at one electrode to the current i_o at the other electrode, see Figure 1c:

$$i_o = \frac{v_b}{Z_s || Z_p}, \tag{2}$$

with $||$ the parallel operator, i.e. $Z_a || Z_b = \left(Z_a^{-1} + Z_b^{-1}\right)^{-1}$, and impedance $Z_n = 1/(j\omega C_n)$. The handle layer voltage v_b is:

$$v_b = i_i \left(Z_b || Z_s || Z_p\right), \tag{3}$$

and the the total current is:

$$i_i = \frac{v_i}{Z_s || Z_p + Z_b || Z_s || Z_p}. \tag{4}$$

Substitution leads to an expression for the impedance from v_i to i_o:

$$Z_m = \frac{v_i}{i_o} = \frac{2(C_s(\varepsilon_r) + C_p) + C_b}{j\omega(C_s(\varepsilon_r) + C_p)^2} = \frac{1}{j\omega C_m}, \tag{5}$$

or:

$$C_m = \frac{(C_s(\varepsilon_r) + C_p)^2}{2(C_s(\varepsilon_r) + C_p) + C_b}. \tag{6}$$

FABRICATION

The fabrication of the device is based on surface channel technology, comprehensively described in [9] and [10]. The specific technology for this device uses a highly conductive silicon-on-insulator wafer (Figure 2a). A silicon nitride layer is deposited on both sides of the wafer using low pressure chemical vapor deposition (Figure 2b). Inlets are etched at the bottom using deep reactive ion etching and stop at the buried oxide layer (Figure 2c). To realize the channel, a slit pattern is etched in the silicon nitride layer (Figure 2d), then, an isotropic etch forms the channel outline in the silicon (Figure 2e). The buried oxide layer is etched between the channel and the inlet with hydrogen fluoride. A second silicon nitride deposition step forms the channel walls and seals the ceiling of the channel (Figure 2g). Pits are etched through the silicon nitride (Figure 2h) to allow the sputtered chromium/gold layer (Figure 2h) to make electrical contact with the silicon device layer. Using reactive ion beam etching, the gold is patterned (Figure 2j). The channels and the silicon electrodes are released using isotropic etching in the silicon device layer (Figure 2k). More space around the channels could be achieved by etching the buried oxide layer and part of the silicon handle layer (Figure 2l.

Two devices are fabricated using this technology:

- a structure to test the conduction between the metal layer to the silicon layer and the isolation of the silicon electrodes (Figure 3);
- the relative permittivity sensor as described above (Figure 4).

The test structure consists of an isolated silicon island. A metal horizontal wire crosses the island on top of the silicon nitride. A vertical wire consists of a metal track that is connected to the silicon island underneath using the etched pit in the silicon nitride. The vertical and horizontal wires cross without contact. The photomask design is printed in Figure 3.

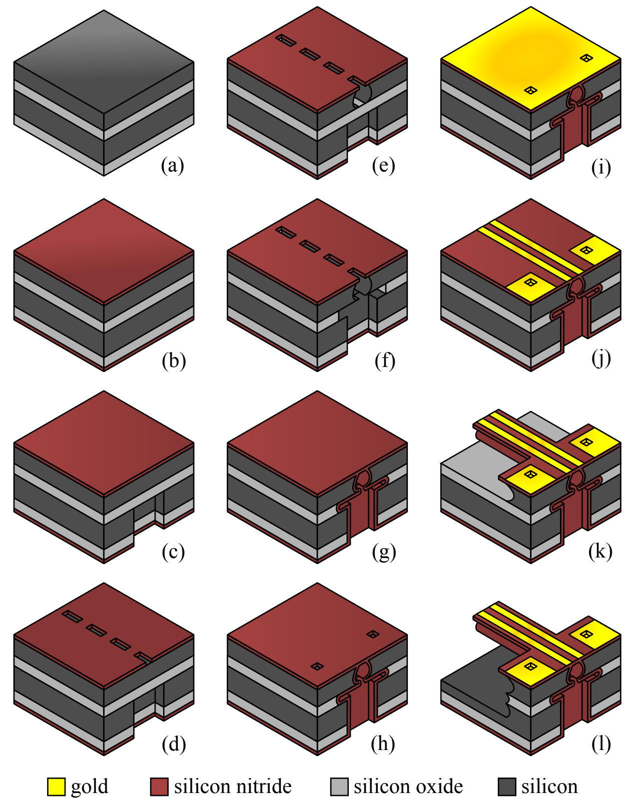

Figure 2: Illustration of the fabrication steps in isometric view. By etching isotropically in silicon through slits in a silicon nitride layer, micro channels are fabricated. The channel walls are realized by applying an extra silicon nitride layer. Metal is deposited for wiring. An isotropic silicon etch releases the channel from the silicon and enables the fabrication of isolated silicon electrodes.

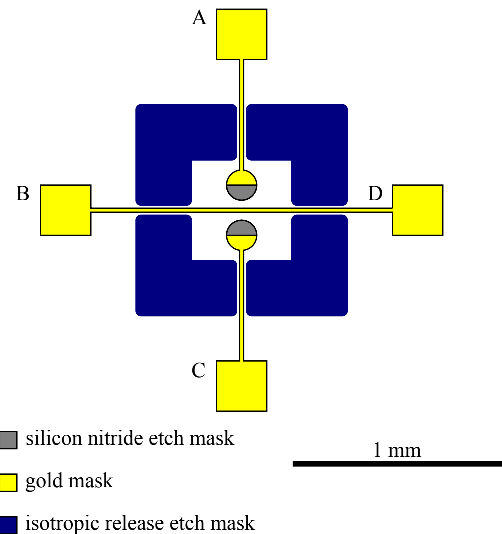

Figure 3: Photomask design for testing the isolation of the silicon electrode, and the conduction from metal layer to silicon. There is a wire between bondpads A and C and between B and D. The wires cross, but should not be connected to eachother.

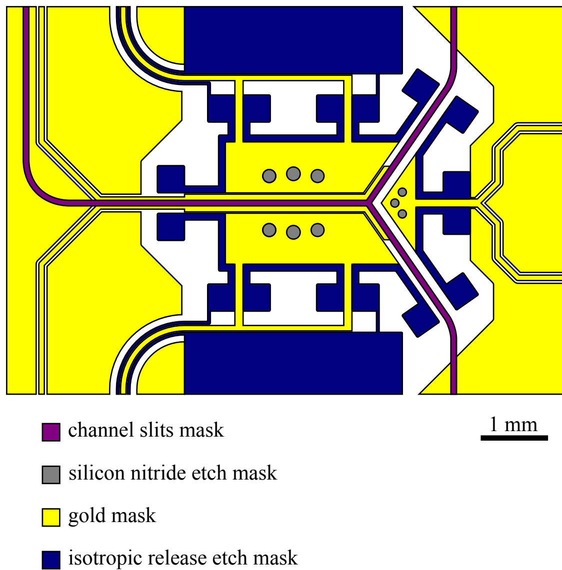

Figure 4: Photomask design of the relative permittivity sensor.

The photomask design of the sensor itself is based on the illustration in Figure 1. The channel splits in two for on-chip mixing purposes, but this feature is not used in the experiments presented in this paper. Figure 4 shows the photomask design. Figure 5 shows a scanning electron microscopy (SEM) image of the fabricated test structure. Figure 6 shows SEM images of the fabricated sensor and a photograph of the sensor assembled on a printed circuit board.

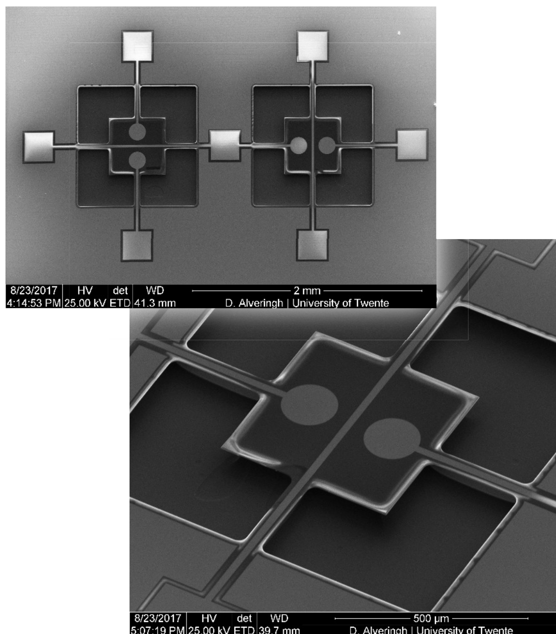

Figure 5: SEM image of the fabricated test structure.

CHARACTERIZATION

Preliminary to the sensor characterization, the isolation of the silicon electrode is checked using the test structure. Besides, the conductivity of the metal to silicon interfaces is tested using the same structure. The resistance between bondpads A and C in Figure 3 was 35 Ω. The resistance between bondpads B and D was similar, 38 Ω.

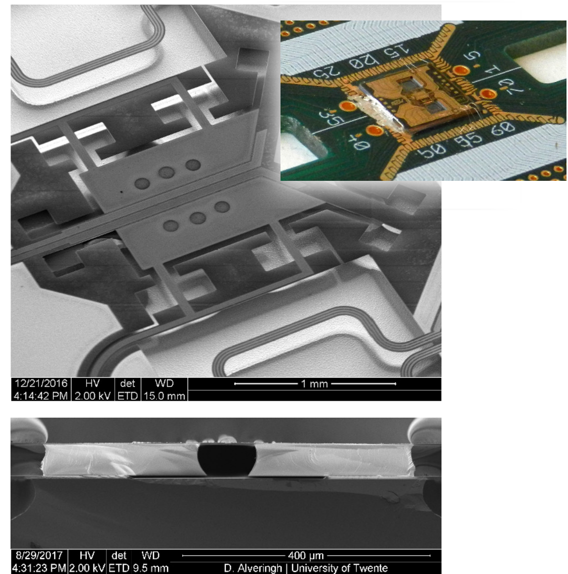

Figure 6: SEM image of the fabricated device and a photograph of the device adhesively mounted to a printed circuit board.

The resistance between bondpads C and D was > 100 MΩ. It can be concluded that the island is well isolated and is addressable by connecting it to an external bondpad.

The sensor is characterized at room temperature using the microfluidic assembly and interfacing method presented in [11] and an HP4194A impedance analyzer with the setup illustrated in Figure 7. Nitrogen, hexane, trichloromethane, propan-2-ol, ethanol and methanol with known relative permittivities [1, 12] are applied using a syringe.

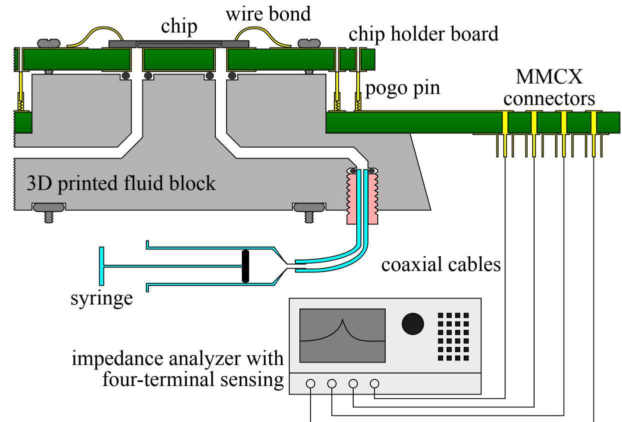

Figure 7: Electric and fluidic interfacing. The chip is mounted to a chip holder board. The chip holder board is electrically connected to a main board and fluidically connected to a 3D printed fluid block. An impedance analyzer is connected to the main board in a four-terminal setup. The fluid block is connected to a syringe.

The magnitudes and phases of the impedances are obtained for all fluids in the frequency range from 1 MHz to 10 MHz with a logarithmic sweep in 401 steps. These magnitudes are plotted in Figure 8. The measured capacitances C_m (using Equation 5) are averaged for all 401 frequency

steps. The resulting capacitance of each fluid is plotted in Figure 9 as a function of relative permittivity. The figure also shows the fitted theoretical response according to Equation 6, with β = 0.82 pF, C_p = 8 pF and C_b = 7.5 nF. These values are in the same order of manitude as estimated by Equation 1 using the measured dimensions from Figure 6.

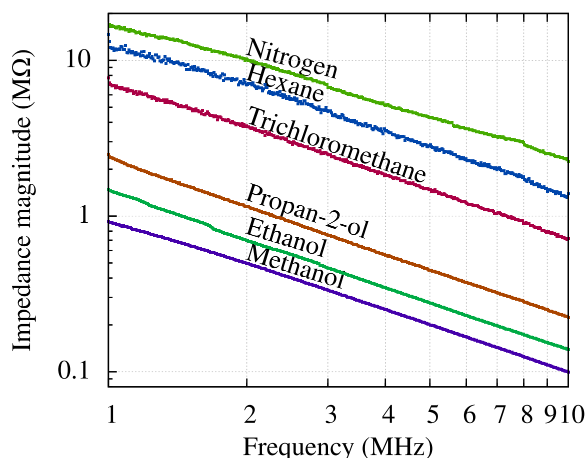

Figure 8: Measured magnitudes of the impedances for different fluids from 1 MHz to 10 MHz.

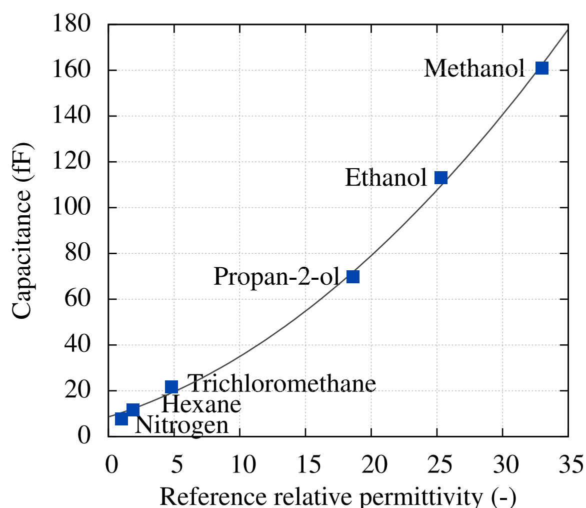

Figure 9: Sensor characterization results against relative permittivity values from literature with model fit.

CONCLUSION

A relative permittivity sensor is designed, fabricated and characterized for different substances. A coefficient of determination of R^2 = 99.83 % with a fitted model is observed. The device enables therefore accurate inline, real-time and non-invasive relative permittivity measurements with low internal volumes.

This is the first device that successfully uses the isolated silicon electrode functionality of surface channel technology. Resistance measurements show that the electrodes are well isolated and could be used for a capacitive readout. Other devices using the same technology can be integrated on a single chip with this device, e.g. flow and pressure sensors.

In future work, the measurement setup will be improved with accurate temperature control, since the relative permittivity of many substances is temperature dependent. By increasing resolution, relative permittivity sensing for gases might be possible. Parasitics (C_p) and drift can be reduced by differential measurements using a second on-chip empty reference sensor.

ACKNOWLEDGEMENTS

The authors gratefully acknowledge support by the Eurostars Programme through the TIPICAL project (E!8264), and Remco Sanders, Henk-Willem Veltkamp and Jarno Groenesteijn for the technical contribution.

REFERENCES

[1] W. M. Haynes, *CRC handbook of chemistry and physics*, 95th ed. CRC press, 2014.

[2] D. Thompson, “Dielectric constant measurement method,” Dec. 11 1973, US Patent 3,778,706.

[3] K. Ogawa *et al.*, “Dielectric constant detecting apparatus,” May 9 1995, US Patent 5,414,368.

[4] I. M. Woodhead *et al.*, “Dielectric constant monitor,” Sep. 15 1992, US Patent 5,148,125.

[5] B. K. Alfredovich *et al.*, “Device for measuring permittivity of materials,” Sep. 26 1972, US Patent 3,694,742.

[6] M. F. Iskander, “Apparatus and method for measuring the permittivity of a substance,” Apr. 9 1985, US Patent 4,510,437.

[7] J. C. Lötters *et al.*, “Fully integrated microfluidic measurement system for real-time determination of gas and liquid mixtures composition,” in *The 18th International Conference on Solid-State Sensors, Actuators and Microsystems (TRANSDUCERS 2015)*. IEEE, 2015, pp. 1798–1801.

[8] R. P. Feynman *et al.*, *Feynman lectures on physics, Volume 2: Mainly electromagnetism and matter*. Reading, Massachusetts, United States of America: Addison-Wesley, 1964.

[9] J. Groenesteijn *et al.*, “A versatile technology platform for microfluidic handling systems, part I: fabrication and functionalization,” *Microfluidics and Nanofluidics*, vol. 21, no. 7, p. 127, July 2017.

[10] J. Groenesteijn *et al.*, “A versatile technology platform for microfluidic handling systems, part II: channel design and technology,” *Microfluidics and Nanofluidics*, vol. 21, no. 7, p. 126, July 2017.

[11] D. Alveringh *et al.*, “Universal modular fluidic and electronic interfacing platform for microfluidic devices,” in *Proceedings of the 3rd Conference on MicroFluidic Handling Systems (MFHS 2017)*, 2017, pp. 106–109.

[12] G. Akerlof, “Dielectric constants of some organic solvent-water mixtures at various temperatures,” *Journal of the American Chemical Society*, vol. 54, no. 11, pp. 4125–4139, 1932.

CONTACT

Dennis Alveringh
d.alveringh@utwente.nl